Environmental Science & Technology

Article

Cite This: Environ. Sci. Technol. 2019, 53, 9926−9936

pubs.acs.org/est

In Situ Photoelectrochemical Chloride Activation Using a WO_3 Electrode for Oxidative Treatment with Simultaneous H_2 Evolution under Visible Light

Min Seok Koo,[†] Xiaofang Chen,[‡] Kangwoo Cho,[†] Taicheng An,*[,‡] and Wonyong Choi*[,†]

[†]Division of Environmental Science and Engineering, Pohang University of Science and Technology (POSTECH), Pohang 37673, Korea

[‡]Guangdong Key Laboratory of Environmental Catalysis and Health Risk Control, Institute of Environmental Health and Pollution Control, Guangdong University of Technology, Guangzhou 510006, China

Supporting Information

ABSTRACT: Reactive chlorine species (RCS) such as HOCl and chlorine radical species is a strong oxidant and has been widely used for water disinfection. This study investigated a photoelectrochemical (PEC) method of RCS production from ubiquitous chloride ions using a WO_3 film electrode and visible light. The degradation of organic substrates coupled with H_2 evolution using a WO_3 electrode was compared among electrochemical (EC), photocatalytic (PC), and PEC conditions (potential bias: +0.5 V vs Ag/AgCl; λ > 420 nm). The degradation of 4-chlorophenol, bisphenol A, acetaminophen, carbamazepine, humic acid, and fulvic acid and the inactivation of *E. coli* were remarkably enhanced by in situ RCS generated in PEC conditions, whereas the activities of the PC and EC processes were negligible. The activities of the WO_3 film were limited by rapid charge recombination in the PC condition, and the potential bias of +0.5 V did not induce any significant reactions in the EC condition. The PEC activities of WO_3 were limited in the absence of Cl^- but significantly enhanced in the presence of Cl^-, which confirmed the essential role of RCS in this PEC system. The PEC mineralization of organic compounds was also markedly enhanced in the presence of Cl^- where dark chemical chlorination by NaOCl addition induced a negligible mineralization. The H_2 generation was observed only at the PEC condition and was negligible at PC and EC conditions. On the other hand, the oxidation of chloride on a WO_3 photoanode produced chlorate (ClO_3^-) as a toxic byproduct under UV irradiation, but the visible light-irradiated PEC system generated no chlorate.

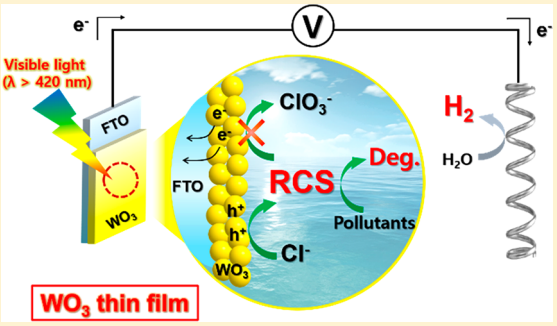

INTRODUCTION

Active chlorine is widely used for chemical oxidation of ammonia, disinfection of drinking water, swimming pools, and wastewater, owing to the proper oxidation power and relatively long lifetime.[1−4] Chloride ion can be oxidized to reactive forms such as hypochlorous acid (HOCl), hypochlorite ion (OCl^-), Cl_2, and chlorine radicals (Cl•, $Cl_2^{\bullet-}$), which are collectively referred to as reactive chlorine species (RCS) throughout this manuscript. These RCS have a strong oxidizing power enough to oxidize various organic pollutants and inactivate microorganisms. The relative amount of each RCS form is dependent on pH. Dissolved chlorine gas (Cl_2 (aq)) is preferred at an acidic condition (pH < 3.3), which is subsequently hydrolyzed to HOCl as a main RCS form at 3.3 < pH < 7.5 (eq 5), while OCl^- is the main species at pH > 7.5 (eq 6).[5] The disinfection power of HOCl is generally regarded to be higher than that of OCl^- by 80−100 times.[5] Therefore, HOCl plays an important role in water treatment under acidic conditions.

Chlorination in electrochemical and UV photochemical systems has been studied extensively.[6−10] However, the chlorination methods that generate RCS by activating ubiquitous chloride ions without the need (or with the minimal need) of electricity and UV light source are highly desired in terms of the process safety and cost. This study is motivated by the need of RCS generation using only visible light and economical photoelectrode material. The photoelectrochemistry (PEC) of semiconductor metal oxides has been intensely investigated for not only solar fuel production but also the generation of reactive oxygen species (ROS) for water treatment over the past decades.[11−13] A recent study successfully demonstrated the dual-functional PEC process, employing a TiO_2 photoanode and a stainless steel cathode, which generates •OH radicals on the photoanode and reduces

Received: April 19, 2019
Revised: July 12, 2019
Accepted: July 17, 2019
Published: July 18, 2019

Downloaded via GUANGDONG UNIV OF TECHNOLOGY on October 9, 2019 at 06:33:43 (UTC).
See https://pubs.acs.org/sharingguidelines for options on how to legitimately share published articles.

© 2019 American Chemical Society

DOI: 10.1021/acs.est.9b02401
Environ. Sci. Technol. 2019, 53, 9926−9936

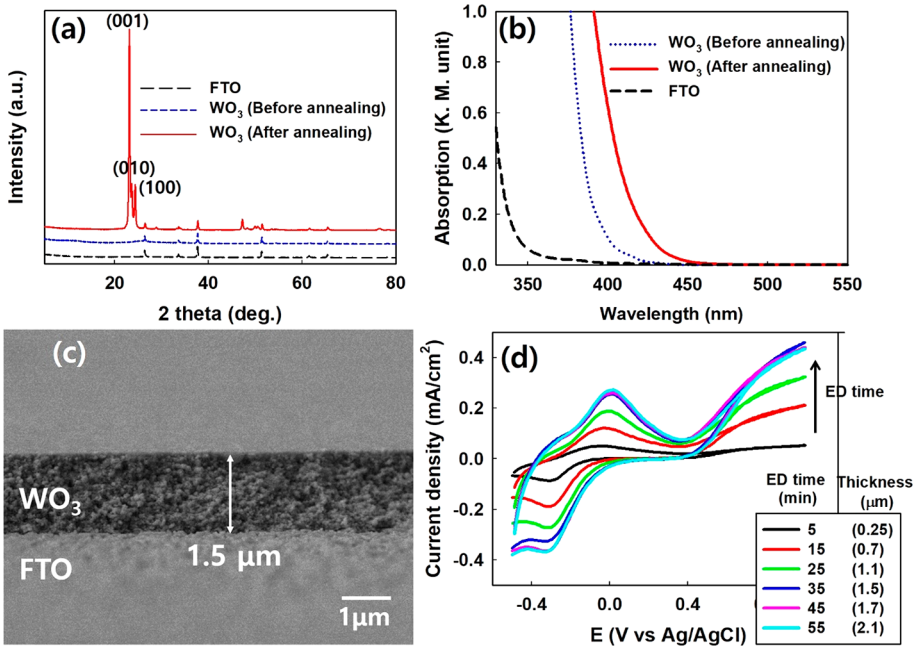

Figure 1. (a) XRD patterns and (b) DRS spectra of WO_3 before and after the annealing process. (c) The cross-sectional image of a WO_3 thin film electrode. (d) The cyclic voltammograms of WO_3 thin film electrodes with different electrodeposition (ED) times under visible light irradiation. [Na_2SO_4] = 0.1 M, [NaCl] = 50 mM, pH 4, λ > 420 nm.

water to molecular hydrogen on the cathode simultaneously.[14] However, since TiO_2 that cannot absorb visible light is not an efficient photoelectrode for solar light utilization, visible light absorbing WO_3 with a band gap of approximately ~2.8 eV[15] and valence band (VB) edge located at ~3.0 V (vs NHE)[16] has been frequently investigated. Owing to the relatively low cost and stability in acidic conditions, WO_3 has been widely used as a popular photoanode material for solar conversion processes such as water photooxidation and water purification.[17−19] The formation of a WO_3 thin film electrode has been investigated by electrodeposition,[18] the sol−gel method,[20] the vacuum coating method,[21] and the doctor blade method.[22] Above all, a WO_3 thin film made by the electrodeposition method exhibited superior electrochromic properties and higher PEC activity and could be easily prepared on large area electrodes.[23]

Herein, we proposed and investigated a WO_3-based PEC system which achieved the degradation of organic compounds (or microbial inactivation) by RCS and the production of H_2 simultaneously under visible light irradiation. In particular, the present visible-light PEC system produced no toxic chlorination byproducts such as ClO_3^- and ClO_4^-, which are commonly generated from UV-photooxidation[24] and electrochemical oxidation[25] of chloride. This study demonstrates an attractive strategy for utilizing ubiquitous chloride for water purification and an energy-recovering process using immobilized catalysts and solar light.

MATERIALS AND METHODS

Electrodes Preparation and Characterization. Tungsten trioxide thin films were prepared through an electrochemical deposition on a conducting FTO glass substrate (Pilkington, 15 Ω per square) as reported previously.[26] Tungsten powder (2.0 g) was dissolved in a hydrogen peroxide solution (10 mL, Junsei, 35% purity). After the exothermic reaction ended, 100 mL of distilled water and 30 mL of isopropyl alcohol were added in solution. A cleaned Pt wire was immersed in the prepared solution for several hours to decompose residual hydrogen peroxide in solution. The electrochemical deposition was carried out with the three-electrode configuration, which included a working electrode (FTO glass, 1 × 2 cm^2), a Pt wire as a counter electrode, and a Ag/AgCl reference electrode. A potential of −0.4 V (vs Ag/AgCl) was applied to the working electrode for 35 min. At the end of the deposition process, a potential of 0.2 V (vs Ag/AgCl) was applied on the working electrode to remove the blue coloration caused by the electron accumulation on WO_3 during the deposition process. The obtained WO_3 thin film was carefully washed with ethanol and distilled water and then annealed in air for 1 h at 450 °C. A WO_3 thin film was characterized by field emission scanning electron microscopy (FE-SEM, JEOL, JSM-7401F), diffuse reflectance spectroscopy (DRS, Shimadzu UV-2401PC), and X-ray diffraction (XRD, Max Science Co., M18XHF) using Cu−Kα radiation. A boron-doped diamond (BDD) electrode (WESCO electrode) was used as a control electrode for comparing the PEC and electrochemical treatments.

(Photo)Electroanalytical Measurements. A single compartment cell (working volume: 50 mL) with the three-electrode configuration was employed in this study, which included a working electrode (WO_3 thin film, 1 × 2 cm^2), a Pt wire as a counter electrode, and a Ag/AgCl reference electrode. The electrode module was connected to a computer-controlled potentiostat (Gamry Instruments Reference 600). The supporting electrolyte for the following measurements was 0.1 M Na_2SO_4 solution. Cyclic voltammetry (CV) data were collected in the potential range of −0.5 to +1.0 V (vs Ag/AgCl) at a scan rate of 50 mV s^{-1}. For visible light irradiation, a 300-W Xe arc lamp with a cutoff filter (λ > 420 nm) was used as a light source.

Degradation of Organic Substrates Coupled with H_2 Generation. The degradation of organic substances and concurrent H_2 generation were conducted in a single

DOI: 10.1021/acs.est.9b02401
Environ. Sci. Technol. 2019, 53, 9926−9936

compartment cell reactor (working volume: 50 mL) with the three-electrode system, which included a working electrode (WO_3 thin film, 1 × 2 cm^2), a counter electrode (Pt wire), and a reference electrode (Ag/AgCl). The potential bias was fixed at +0.5 V vs Ag/AgCl (+0.7 V_{NHE}), and the visible irradiation (λ > 420 nm) source was the 300-W Xe arc lamp. The incident light intensity was measured by an optical power meter (Newport 1918-R), and the intensity of visible light active for exciting WO_3 (i.e., 420−455 nm region, see Figure 1b) was estimated to be about 15 mW/cm^2 by light intensity measurements using two long-pass filters (transmitting at λ > 420 and λ > 455 nm, respectively). 4-Chlorophenol (4-CP, Sigma), bisphenol A (BPA, Sigma), acetaminophen (AAP, Sigma), carbamazepine (CBZ, Sigma), and humic acid and fulvic acid (HA, FA, Suwannee River) were chosen as target organic substrates to compare their degradation efficiencies in variable energy input conditions: electrochemical (EC, potential bias only), photocatalytic (PC, irradiation only), and photoelectrochemical (PEC, potential bias with irradiation). The initial substrate concentrations were 50 μM for 4-CP, BPA, AAP, and CBZ and 1 ppm for FA and HA, while 0.1 M Na_2SO_4 was added as a supporting electrolyte (with or without 50 mM NaCl). Coumarin (Sigma) was used as a trapping reagent of OH radicals, and *tert*-butyl alcohol (TBA, Sigma),[15] ethylenediaminetetraacetic acid (EDTA, Sigma),[27] and sodium thiosulfate ($Na_2S_2O_3$, Sigma)[25] were used as OH radical, hole, and residual RCS scavenger, respectively. For the measurement of H_2 gas evolution, the reactor with 0.1 M Na_2SO_4 electrolyte (with or without 50 mM NaCl) and organic substrate (4-CP) was initially purged with Ar gas (Linde, 99.9995%) for 1 h to remove the dissolved oxygen. During the reaction, gas samples were periodically withdrawn from the headspace with a 100 μL glass syringe (Hamilton 81030).

Bacterial Inactivation. *E. coli* K12 (The Coli Genetic Stock Center at Yale University, USA) was selected as the model bacterial strain to evaluate the PEC (with or without 50 mM NaCl), PC, and EC disinfection. The bacterial strains were stored in 25% sterilized glycerin at −80 °C. To prepare the bacterial suspension for inactivation, the individual bacterial strain was streaked on a nutrient agar plate and incubated to acquire isolated colonies. Bacterial strains were cultured in nutrient broth at 37 °C for 16 h with shaking 200 rpm to log phase. The cells were successively harvested by centrifugation at 4000 rpm for 15 min, washed twice with 0.01 M PBS, and then moved to 50 mL 0.1 M Na_2SO_4 (pH = 4.0, adjusted with H_2SO_4). The cell concentration was adjusted to a final cell density of 10^7 cfu mL^{-1}, and the PEC bacterial inactivation experiments were conducted under a constant applied potential of +0.5 V (vs Ag/AgCl) in a 50 mL three-electrode PEC bulk reactor. Before each experiment, the reactor was washed several times to remove the residual organics generated from the decomposition of bacteria, and all glassware were sterilized by autoclaving at 120 °C for 15 min. The reaction temperature was maintained at about 25 °C, and the reaction solution was mixed under magnetic stirring throughout the experiment. At different time intervals, 1.5 mL aliquots were collected for further analysis of final bacterial survival by diluting with sterilized 0.01 M PBS solution and spreading 0.1 mL of the diluted sample uniformly on nutrient agar plates. The nutrient agar plates were incubated at 37 °C for 16 h, and the colonies formed were counted before and after the inactivation experiment. Each experiment was conducted in triplicates.

Analytical Methods. The concentration of free chlorine species (FCS mainly as HOCl, excluding chlorine radical species generated in the PEC system) was measured using the DPD (*N*,*N*-diethyl-*p*-phenylenediamine) colorimetric method[28] by measuring the absorbance at 515 nm with a UV/visible spectrophotometer (Libra S22, Biochrom). The current efficiency (η_{FCS}) of FCS generation (eq 1) was estimated in the single compartment cell and calculated from eq 2

$$Cl^- + H_2O \rightarrow HOCl + H^+ + 2e^- \quad (1)$$

$$\eta_{FCS}\,(\%) = \frac{2FV}{I} \times \frac{d[FCS]}{dt} \times 100 \quad (2)$$

where F is the Faraday constant (96485 C mol^{-1}), V is the electrolyte volume (0.05 L), [FSC] is the concentration of HOCl and OCl^- (M), I is the current (A), and t is the reaction time (s). Chlorate (ClO_3^-) was analyzed using an ion chromatograph (IC, Dionex ICS-2100) which was equipped with a column Dionex IonPac AS 18 (4 mm × 250 mm) and a conductivity detector. Analysis of 4-CP, BPA, AAP, CBZ, and the degradation intermediates was done using a high-performance liquid chromatograph (HPLC, Agilent 1100). HA and FA were analyzed by monitoring their fluorescence emission using a spectrofluorometer (HORIBA fluoromax-4) under the excitation of 279 nm. H_2 in gas samples was analyzed by a gas chromatograph (GC, HP6890A) with a thermal conductivity detector (TCD) and a 5 Å molecular sieve column.

RESULTS AND DISCUSSION

Properties of Electrodeposited WO_3 Thin Film. Figure 1a shows the XRD patterns of WO_3 thin films before and after the annealing process at 450 °C for 1 h in air. Before the annealing process, an amorphous phase of WO_3 deposited on FTO glass exhibited no XRD patterns (almost the same with bare FTO glass), but the annealing treatment transformed the amorphous WO_3 into a crystalline phase with inducing markedly enhanced XRD intensities. The outstanding diffraction peaks at 23.1°, 23.7°, and 24.2° (2θ) correspond to the (001), (010), and (100) crystal planes of WO_3.[29] The DRS in Figure 1b shows a red-shift of the spectrum and greater absorption of visible light for the crystalline WO_3 after the annealing process. The band gap of amorphous WO_3 (3.05 eV) was reduced to 2.82 eV after the annealing process (Figure S2). The film thickness increased gradually along with the electrodeposition (ED) time, with increasing from 0.25 to 2.1 μm when the ED time increased from 5 to 55 min (Figure S1). The optimal thickness of a WO_3 thin film was determined by monitoring the photocurrent response during cyclic voltammetry (CV) analysis and found to be around 1.5 μm (Figure 1c and 1d). The anodic photocurrent generated on WO_3 under visible light irradiation increased with increasing ED time up to 35 min (resulting in 1.5 μm thickness), and a further increase of ED time slightly increased the photocurrent thereafter (Figure 1d). Since the light penetration depth of WO_3 has been previously estimated to be ∼2.2 μm at 420 nm,[30] the optimal thickness was set to be lower than the penetration depth so that the whole mass of the deposited WO_3 could effectively absorb photons.

FCS Generation on WO_3 under Visible Light. The production of FCS on WO_3 was measured and compared

DOI: 10.1021/acs.est.9b02401
Environ. Sci. Technol. 2019, 53, 9926−9936

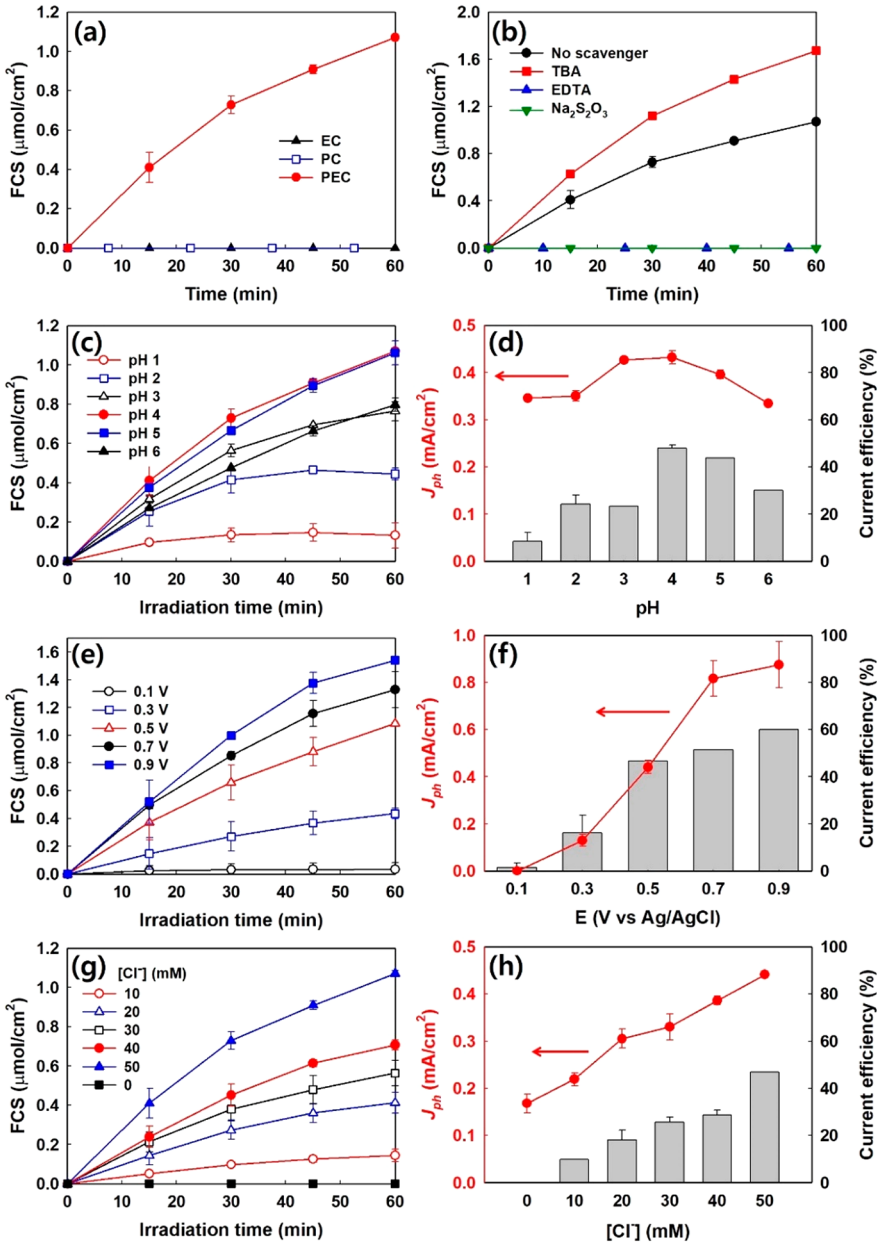

Figure 2. (a) Production of free chlorine species (FCS) on a WO_3 thin film electrode in PEC, PC, and EC conditions. (b) The effect of TBA, EDTA, and $Na_2S_2O_3$ addition on the generation of FCS on a WO_3 thin film electrode. +0.5 V (vs Ag/AgCl), $[Na_2SO_4]$ = 0.1 M, [NaCl] = 50 mM, $[TBA]_0$, $[EDTA]_0$, and $[Na_2S_2O_3]$ = 0.1 M, pH 4, λ > 420 nm. Effect of (c) pH, (e) applied potential (vs Ag/AgCl), and (g) chloride concentration on the FCS generation on a WO_3 thin film electrode under visible light irradiation (λ > 420 nm). Photocurrent density and current efficiency of FCS generation depending on (d) pH, (f) applied potential (vs Ag/AgCl), and (h) chloride concentration. $[Na_2SO_4]$ = 0.1 M, λ > 420 nm. The FCS generation of 1 μmol/cm^2 corresponds to [FCS] = 0.04 mM.

among the different operation conditions of PEC, PC, and EC (Figure 2a). Only the PEC condition generated FCS, and the EC and PC conditions could not generate FCS at all because the applied potential (+0.5 V vs Ag/AgCl) in the EC condition was lower than the minimum potential required for chloride oxidation (+1.36 V_{NHE}) and the PC condition without a potential bias was not efficient in separating charge pairs. However, in the PEC condition, FCS was effectively generated since the applied potential bias can assist the separation of the charge pairs. To investigate the FCS generation mechanism in the PEC condition, TBA, EDTA, and $Na_2S_2O_3$ were used as scavengers for •OH, holes, and FCS, respectively, in the PEC condition (Figure 2b). In the presence of either EDTA or $Na_2S_2O_3$, the generation of FCS was completely inhibited, which indicated that the FCS generation is mediated by hole oxidation of chloride ion. However, it is interesting to note that the FCS generation rate was even enhanced in the presence of TBA. This implies that some hydroxyl radicals generated on a WO_3 photoanode (via eq 3) may transform HOCl into inactive chlorine species such as chlorite and chlorate (e.g., see eqs 10–13). When OH radicals are scavenged by TBA, the further transformation of HOCl can be inhibited to increase the level of FCS.

The FCS generation in the PEC condition was optimized with varying pH, applied potential bias, and concentration of chloride ion under visible light (see Figure 2c–2h). The

DOI: 10.1021/acs.est.9b02401
Environ. Sci. Technol. 2019, 53, 9926–9936

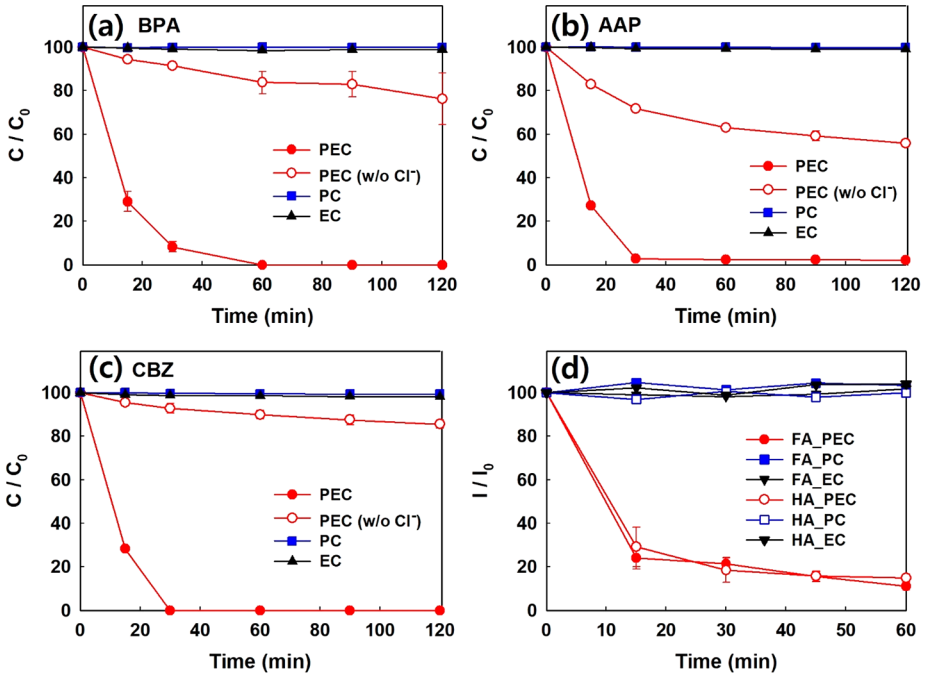

Figure 3. Time profiles of (a) bisphenol A (BPA), (b) acetaminophen (AAP), and (c) carbamazepine (CBZ) degradation on a WO_3 thin film electrode in PEC, PC, and EC conditions. (d) Time profiles of the fluorescence emission intensity (excited at λ_{ex} = 279 nm) of fulvic acid (FA: λ_{em} = 451 nm) and humic acid (HA: λ_{em} = 464 nm) in PEC, PC, and EC conditions. C_0 = 50 μM, $[FA]_0$ and $[HA]_0$ = 1 ppm, $[Na_2SO_4]$ = 0.1 M, [NaCl] = 50 mM, +0.5 V (vs Ag/AgCl), λ > 420 nm, pH = 4.

generation of FCS was monitored every 15 min in the PEC system under visible light irradiation (λ > 420 nm). The effect of pH on FCS generation (Figure 2c) was investigated in the pH range of 1 to 6 with 50 mM NaCl. The FCS generation rate was the highest around pH 4 and reduced below and above pH 4. The η_{FCS} was below 30% from pH 1 to 3 and sharply increased to about 50% at pH 4 (Figure 2d). The rest of the photocurrent seemed to be consumed in the oxygen evolution reaction (OER) from water oxidation. At pH 1−3, FCS is present mainly as Cl_2 which can be removed through volatilization with reducing the current efficiency of FCS generation. As the pH increased beyond pH 4, η_{FCS} is reduced probably because the VB edge potential moves to the negative direction with increasing pH, which should reduce the driving force of chloride oxidation (eq 4). In addition, the surface of WO_3 is negatively charged above pH 4 since the point of zero charge (PZC) of WO_3 is 4−5,[16,31] which should inhibit the adsorption of Cl^- on a WO_3 electrode and decrease the formation of RCS. It should be also noted that the WO_3 thin film is stable only in acidic conditions,[32] where WO_3 is dissolved as WO_4^{2-} above pH 6. This might be also responsible for the reduced FCS production at pH 6.

$$h^+_{VB} + H_2O \rightarrow \bullet OH, \quad E^0 = 2.8\ V\ (vs\ NHE) \tag{3}$$

$$2h^+_{VB} + 2Cl^- \rightarrow Cl_2(aq) \tag{4}$$

$$Cl_2(aq) + H_2O \leftrightarrow HOCl + HCl \tag{5}$$

$$HOCl \leftrightarrow OCl^- + H^+ \quad (pK_a = 7.5)^5 \tag{6}$$

As the applied potential bias increased from 0.1 to 0.9 V (vs Ag/AgCl), the FCS production also increased in 50 mM NaCl solution at pH 4 (Figure 2e). A higher anodic potential bias would be more efficient in preventing the recombination of excited charge pairs, as demonstrated by the higher photocurrent density at higher potentials. However, a WO_3 photoanode was less stable at higher bias potential, and the cyclic voltammetry of a WO_3 electrode at 0.7 to 0.9 V exhibited noticeable reduction of photocurrent with repeating the CV cycles (Figure S3). This can be ascribed to the electrode instability of WO_3 at a higher potential bias. At the applied potential of 0.5 V, the photocurrent was maintained relatively stable (Figure S3). As for the chloride concentration effect, increasing $[Cl^-]$ from 10 to 50 mM monotonously increased the FCS concentration (Figure 2g). Chloride ions rapidly react with holes, retarding the recombination of the charge pairs, to increase both the photocurrent density and η_{FCS} (Figure 2h).

Degradation of Organic Compounds and Inactivation of *E. coli*. The activities of photogenerated RCS were tested for the degradation of model organic compounds (4-CP, BPA, AAP, CBZ, HA, and FA) under the operation conditions of PEC, PC, and EC. Figures 3a−3c show that the degradation of model compounds (BPA, AAP, and CBZ) was negligible in EC and PC conditions and observed only in the PEC condition, which is consistent with the FCS generation results shown in Figure 2a. Although the organic substrates could be degraded in a limited extent even in the absence of chloride by direct hole oxidation, the presence of chloride markedly enhanced their degradation, which confirms the essential role of RCS as a main oxidant in the visible light-irradiated PEC system. The PEC degradation rate constants with and without chloride are compared in Table S1. The PEC degradation constants with chloride are higher by an order of magnitude than those without chloride. Analogous results were also obtained for the degradation of FA and HA using a WO_3 thin film. Figure 3d shows the time-dependent variations of FA and HA concentrations, which were expressed in terms of the fluorescence emission intensity (at 451 nm for FA and at 464

DOI: 10.1021/acs.est.9b02401
Environ. Sci. Technol. 2019, 53, 9926−9936

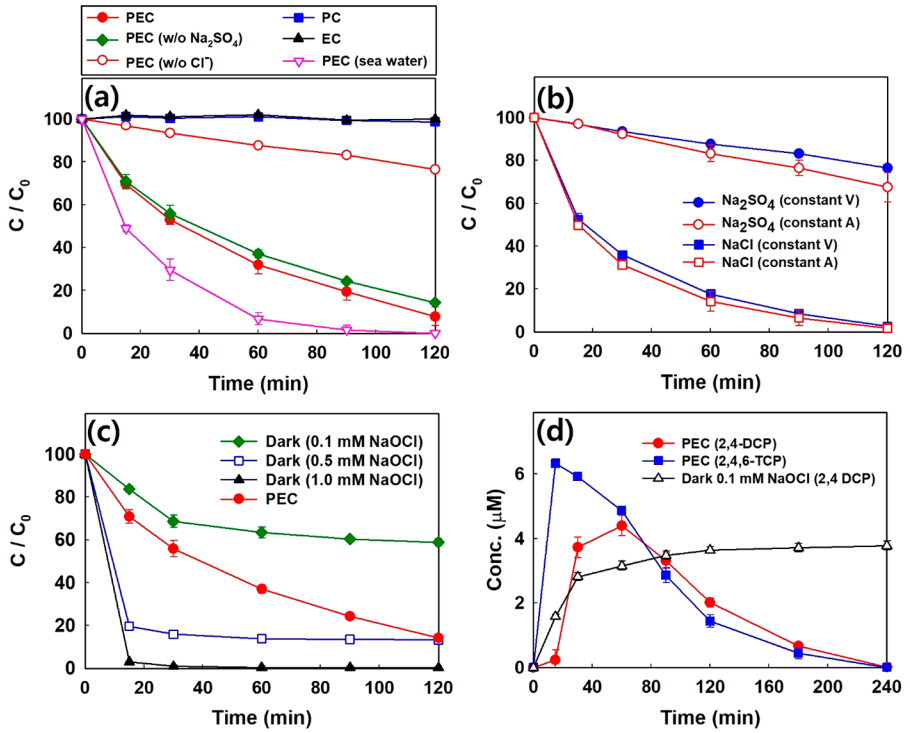

Figure 4. (a) Time profiles of 4-chlorophenol (4-CP) degradation on a WO_3 film electrode in PEC, PC, and EC conditions. (b) Time profiles of 4-CP degradation in 0.1 M of Na_2SO_4 or NaCl with constant potential (0.5 V vs Ag/AgCl) and constant current (0.5 mA/cm^2) in the PEC condition. (c) Comparison of 4-CP degradation between the PEC system with in situ RCS generation and the dark system with initially added NaOCl. (d) Time profiles of the chlorinated intermediates (2,4-dichlorophenol (2,4-DCP) and 2,4,6-trichlorophenol (2,4,6-TCP)) concentrations with PEC and dark chemical chlorination. $[4\text{-CP}]_0$ = 50 μM, [NaCl] = 50 mM, +0.5 V (vs Ag/AgCl), λ > 420 nm, pH = 4.

nm for HA, Figure S4). The degradation of the FA and HA was negligible in EC and PC conditions but markedly enhanced in the PEC condition with chloride ions, which is consistent with the results obtained with the model organic compounds. While the current density in the EC condition was negligible at the applied potential bias of 0.5 V vs Ag/AgCl, it was substantially increased in the PEC condition (Figure S5). The addition of chloride ion further elevated the PEC current density (Figure S5).

It should be mentioned that the PEC performance was demonstrated in the presence of high electrolyte concentration (0.1 M Na_2SO_4) to ensure the solution conductivity high enough for reliable measurements of PEC parameters. However, it is obvious that such reaction conditions are not realistic at all for water treatment. Therefore, the PEC performance was also tested in the absence of Na_2SO_4 electrolyte to demonstrate that the PEC degradation efficiency is little hindered even in the absence of electrolyte (Figure 4a). The PEC degradation with the electrolyte alone (0.1 M Na_2SO_4, without Cl^-) was very limited. More importantly, the PEC mineralization efficiency was not reduced either by the absence of 0.1 M Na_2SO_4 (see Figure 5a). This confirms that the addition of electrolytes (0.1 M Na_2SO_4) that was employed for facile PEC measurements does not affect the organic degradation efficiency. Incidentally, the PEC performance for the organic degradation was tested in real seawater (0.53 M Cl^- without any additional electrolyte) as well, which demonstrated much higher activity than that in the typical PEC condition with 50 mM NaCl (Figure 4a). The present PEC system should be most suitable to the treatment of acidic waters with high chloride content.

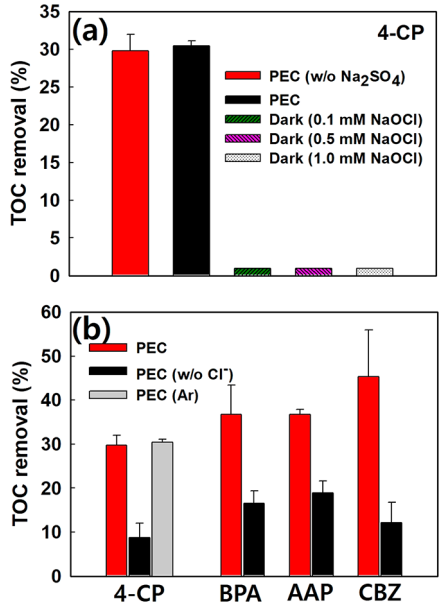

Figure 5. (a) TOC removal efficiency of 4-CP in dark chemical chlorination and in PEC system (with or without Na_2SO_4) using a WO_3 film electrode after 6 h reaction. (b) TOC removal efficiency of organic pollutants (4-CP, bisphenol A (BPA), acetaminophen (AAP), and carbamazepine (CBZ)) (6 h reaction) with or without chloride ion and without dissolved O_2 (Ar-saturated condition) in the PEC system. C_0 = 50 μM, $[Na_2SO_4]$ = 0.1 M, [NaCl] = 50 mM, +0.5 V (vs Ag/AgCl), λ > 420 nm, pH = 4.

As for the pH effect, the PEC system was stable only at acidic conditions (pH 4) and rapidly loses its activity at pH 6

DOI: 10.1021/acs.est.9b02401
Environ. Sci. Technol. 2019, 53, 9926−9936

during repeated uses (Figure S6), which is ascribed to the well-known instability of WO_3 at higher pH.[32] Although the use of a WO_3 electrode is not suitable for neutral and alkaline water, it can be applicable to the treatment of acidic wastewaters. Despite the instability of WO_3 in alkaline conditions, its merits such as low material cost and visible light activity may compensate for the demerit as long as the application is limited to acidic conditions. However, more stable and more efficient visible light-active photoanodes working in a wider pH range should be sought in further studies.

The kinetics of PEC degradation of 4-CP in 0.1 M NaCl solutions was far faster than those in 0.1 M Na_2SO_4 solutions both under potentiostatic and galvanostatic modes (Figure 4b). In addition, the fact that the degradation rates of 4-CP were the same under the potentiostatic and galvanostatic conditions implies that the overall reactions were not limited by surface charge transfer. The photoinduced charge transfer on a WO_3 electrode induces the oxidation of chloride ions to active forms among which $HOCl/OCl^-$ should be the main products as shown in Figure 2. To assess the role of $HOCl/OCl^-$ in the organic degradation, 0.1, 0.5, and 1.0 mM NaOCl (as a form of FCS) were added initially in the absence of NaCl, and the degradation of 4-CP was tested in dark conditions (dark chlorination test in Figure 4c). $Na_2S_2O_3$ as a FCS scavenger was added at each sampling time to prevent further reaction. While the PEC system with in situ RCS generation continuously degraded 4-CP up to 2 h, the degradation of 4-CP under the dark chemical chlorination stopped after all the initially added NaOCl was depleted (Figure 4c). This indicates either that the degradation of 4-CP needs a continuous supply of RCS or that RCS other than $HOCl/OCl^-$ (e.g., chlorine radicals) are involved in the degradation process: both requirements can be met in the PEC system. Note that the added [NaOCl] (0.1−1.0 mM) in the chemical chlorination tests is higher than in situ [$HOCl/OCl^-$] generated in this PEC condition (about 0.04 mM Cl_2 in 1 h). However, the initially added NaOCl is mostly consumed within 20 min of introduction, while RCS is continuously generated in the PEC system to maintain the degradation activity up to 2 h. In particular, it should be noted that dark chemical chlorination alone cannot mineralize organic compounds at all even with the 1.0 mM NaOCl condition (see Figure 5a) under which the parent compound (4-CP) could be completely removed with 30 min (see Figure 4c). Therefore, the main active chlorine species that are responsible for the PEC degradation/mineralization should not be FCS ($HOCl/OCl^-$) but most probably chlorine radicals (Cl•, $Cl_2^{\bullet-}$). Note that RCS in this paper refers to FCS plus chlorine radical species.

TOC removal along with the PEC degradation of the parent compounds was also measured and compared in the absence and presence of chloride. Figure 5b shows that the mineralization of organic substrates in the present PEC system proceeded slowly, and only a partial mineralization was achieved even after a 6 h reaction although the parent organic compounds were completely removed within 2 h. Despite the incomplete TOC removal, the presence of chloride markedly enhanced the TOC removal efficiency in the PEC system (Figure 5b), which is consistent with the positive role of chloride in the PEC removal of parent compounds. Note that the efficiencies of TOC removal (mineralization) were lower than 20% in the absence of chloride (after 6 h PEC reaction), which implies that the direct hole oxidation alone is not efficient in inducing the mineralization. Unlike the dark chemical chlorination, the PEC chlorination system can produce Cl• and $Cl_2^{\bullet-}$ (eqs 7 and 8) which should mineralize organic substances more efficiently. The direct hole oxidation of parent organic compounds and their degradation intermediates may help the mineralization process along with the chlorine radical species (eq 9).

$$h_{VB}^{+} + Cl^{-} \rightarrow Cl\bullet \quad (7)$$

$$Cl\bullet + Cl^{-} \rightarrow Cl_2^{\bullet-} \quad (8)$$

$$h_{VB}^{+} + \text{Org.} \rightarrow \text{Org}_{ox} \rightarrow \rightarrow CO_2 \quad (9)$$

The PEC generation of in situ RCS combined with hole oxidation by utilizing visible light photons only can make solar water treatment technically feasible. In addition, organic compounds degradation in this PEC chlorination system works well even under oxygen-free conditions (Ar-saturated) because the hole-mediated generation of RCS on WO_3 does not require the presence of dioxygen.

On the other hand, the formation of harmful chlorinated intermediates/byproducts in the EC and PEC treatment of organic compounds is of serious concern when the target water contains a high level of chlorides. To address this concern, the formation of the chlorinated intermediates/byproducts from 4-CP degradation was analyzed and compared between the PEC and dark chemical chlorination systems (see Figure S7, Figure 4d). Although some chlorinated intermediates (e.g., 2,4-dichlorophenol) were generated from the degradation of 4-CP in the chloride-containing PEC reactor, they were gradually degraded and eventually removed in the continuing PEC reaction. This is in marked contrast to the dark chemical chlorination case in which 2,4-dichlorophenol was generated as a chlorination byproduct of 4-CP, but it was not removed at all once generated (Figure 4d).

The visible light activated RCS was also tested for the bacterial inactivation. In order to evaluate the bactericidal performance, *E. coli* was selected as the model colony forming bacteria. The dark electrolyte control (without light and potential bias on WO_3) and photolysis control (without a WO_3 electrode) experiments showed no change in the cell density within 4 h (Figure S8). This indicates that the presence of the electrolyte (Na_2SO_4 and NaCl) alone or the visible light (λ > 420 nm) irradiation alone cannot inactivate *E. coli* at all. As shown in Figure 6, the PEC system with chloride ions achieved

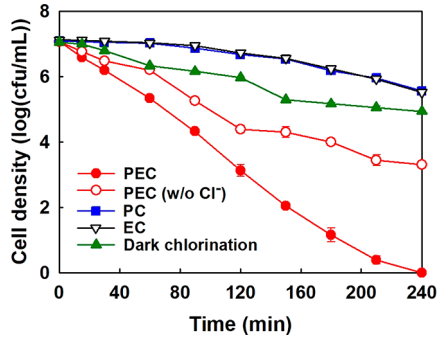

Figure 6. Time-dependent inactivation of *E. coli* in dark chemical chlorination and in PEC, PC, and EC systems employing a WO_3 film electrode. [Na_2SO_4] = 0.1 M, [NaCl] = 50 mM, [NaOCl] = 0.1 mM (for dark chemical chlorination only), +0.5 V (vs Ag/AgCl), λ > 420 nm, pH = 4, the initial cell density of 10^7 cfu mL^{-1}.

DOI: 10.1021/acs.est.9b02401
Environ. Sci. Technol. 2019, 53, 9926−9936

the complete inactivation of bacteria cells within 4 h, whereas lower inactivation efficiencies were obtained in the other conditions: 3.7, 1.6, and 1.7 log reduction in the PEC without chloride, PC and EC conditions, respectively. This observation is consistent with the positive role of Cl^- in degrading organic substances. The visible light-driven PEC chlorination works for bacterial inactivation as well as organic pollutant degradation. The PEC chlorination was far more efficient than the dark chemical chlorination disinfection which was carried out with initially added [NaOCl] that was higher than in situ PEC-generated [$HOCl/OCl^-$] (Figure 6).

Formation of Chlorate and OH Radical. The common byproducts of RCS-mediated oxidation are oxychloro-anions such as chlorite (ClO_2^-), chlorate (ClO_3^-), and perchlorate (ClO_4^-). However, ClO_2^- is hard to be quantified due to the short-lived characteristics (i.e., facile oxidation to ClO_3^-) and analytical limitation.[25] Figure 7a shows the formation of ClO_3^- in the PEC system with 0.1 M Na_2SO_4 and 50 mM NaCl at pH 4, at an applied potential of +0.5 V vs Ag/AgCl under UV (λ > 320 nm) and visible (λ > 420 nm) light irradiation. The

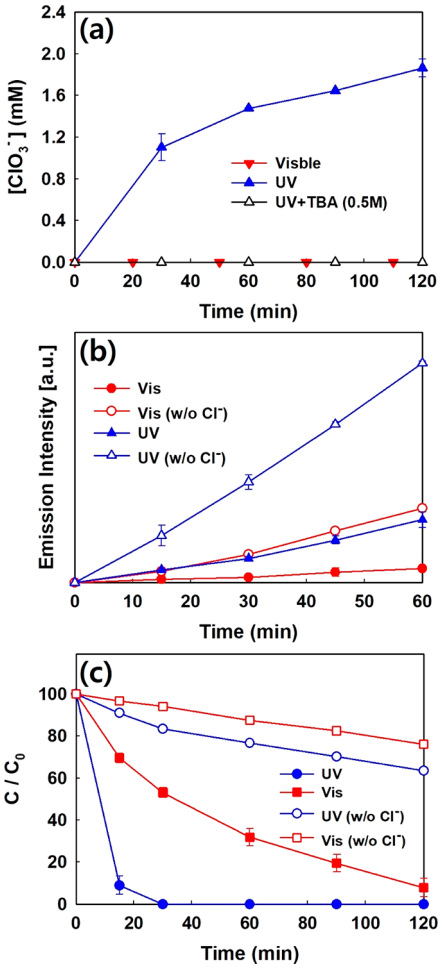

Figure 7. Time profiles of (a) chlorate (ClO_3^-) generation, (b) 7-hydroxycoumarin generation from the reaction of OH radicals with coumarin (1 mM) which was monitored by the fluorescence emission intensity (λ_{em} = 456 nm, excited at 332 nm), and (c) 4-CP degradation in the PEC condition under UV (λ > 320 nm) and visible (λ > 420 nm) light irradiation with or without chloride ion. $[4\text{-CP}]_0$ = 50 μM, [Na_2SO_4] = 0.1 M, [NaCl] = 50 mM, +0.5 V (vs Ag/AgCl), pH = 4.

generation of ClO_3^- was observed only under UV irradiation, which was inhibited by the addition of TBA as an OH radical scavenger. This indicates that the OH radical should be responsible for the formation of ClO_3^-. In the PEC condition, OH radical can be generated by the hole oxidation of water on WO_3 (eq 3). The OH radicals can oxidize chloride sequentially to produce ClO_3^- (eqs 10–13).[33] Since ClO_4^- was not observed at all in our experimental conditions, ClO_3^- was regarded as a stable end product.

$$\bullet OH + HOCl \rightarrow \bullet OCl + H_2O \quad (k = 2.0 \times 10^9\ M^{-1}\ s^{-1}) \tag{10}$$

$$\bullet OH + \bullet OCl \rightarrow ClO_2^- + H^+ \quad (k = 1.0 \times 10^9\ M^{-1}\ s^{-1}) \tag{11}$$

$$\bullet OH + ClO_2^- \rightarrow \bullet ClO_2 + OH^- \quad (k = 6.0 \times 10^9\ M^{-1}\ s^{-1}) \tag{12}$$

$$\bullet OH + \bullet ClO_2 \rightarrow ClO_3^- + H^+ \quad (k = 4.0 \times 10^9\ M^{-1}\ s^{-1}) \tag{13}$$

In order to specify the role of hydroxyl radicals in ClO_3^- formation, we used coumarin as a selective probe reagent for OH radical trapping (Figure 7b). The reaction of coumarin with OH radical would produce 7-hydroxycoumarin (7-HC, eq 14) which could be detected by monitoring its fluorescence emission (Figure S9).[34]

$$\bullet OH + \text{coumarin} \rightarrow \text{7-HC} \quad (\lambda_{em} = 456\ nm) \tag{14}$$

The amount of OH radicals produced under visible and UV light irradiation was significantly enhanced in the absence of chloride ion. This indicates that chloride ions scavenge OH radicals with the concurrent transformation of chloride to RCS. Under visible light irradiation, the PEC generation of OH radicals was insignificant in the presence of chloride. Under UV irradiation, in comparison, the OH radical generation was markedly enhanced even in the presence of chloride ions. Because UV photons are more energetic than visible light photons, more energetic holes (hot holes) are generated under UV irradiation, which should produce OH radicals more efficiently. This is consistent with the observation that chlorate (generated through the action of OH radicals) was produced only under UV irradiation, not under visible light irradiation (see Figure 7a). Although OH radicals seem to play a critical role in oxidizing Cl^- to ClO_3^-, their role in degrading organic substrates appears to be insignificant. While the production of OH radicals was hindered in the presence of Cl^- as shown in Figure 7b, the PEC degradation of a target substrate (4-CP) was greatly enhanced in the presence of Cl^- on the contrary (Figure 7c). This indicates that the main oxidant in the present PEC system is RCS, not OH radical. The RCS generated in this PEC system includes not only $HOCl/OCl^-$ but also chlorine-based radicals (i.e., Cl•, $Cl_2^{\bullet -}$) that are comparable with OH radical. For example, the bimolecular reaction rate constant of OH radical with phenol (k(OH) = 6.6×10^9) can be compared with those of RCS with phenol: k(Cl•) = 2.5×10^{10}, $k(Cl_2^{\bullet -})$ = 2.5×10^8, k(HOCl) = 2.19×10^4.[6] The reactive chlorine and chlorine radical species can serve as effective oxidants in the absence of OH radicals.

H_2 Generation Coupled with PEC Degradation. Figure 8a shows the production of H_2 (in 0.1 M Na_2SO_4 solution with 50 mM NaCl) coupled with the simultaneous degradation of organic substrate (4-CP). In PC and EC conditions, not only the degradation of 4-CP but also H_2 evolution was negligible. Under the PC condition (visible light irradiation only), the fast charge recombination in the unbiased WO_3 film seems to

DOI: 10.1021/acs.est.9b02401
Environ. Sci. Technol. 2019, 53, 9926–9936

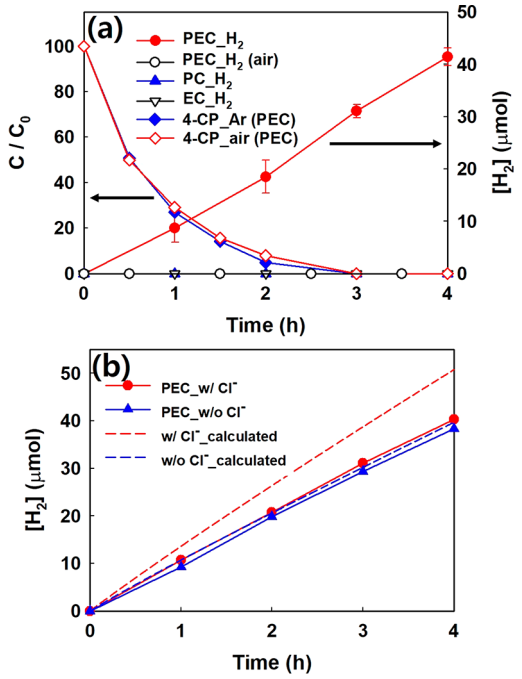

Figure 8. (a) Production of H_2 coupled with 4-CP degradation on a WO_3 thin film electrode in PEC, PC, and EC conditions. (b) Production of H_2 in the PEC condition with or without chloride ion. The dashed lines represent the theoretical amount of H_2 generation based on the measured current with assuming Faradaic efficiency of unity. $[4\text{-CP}]_0$ = 50 μM, $[Na_2SO_4]$ = 0.1 M, [NaCl] = 50 mM, +0.5 V (vs Ag/AgCl for PEC and EC), λ > 420 nm, pH = 4.

inhibit the efficient interfacial charge transfer. In addition, the conduction band position of WO_3 (~0.4 V vs NHE)[35] is not suitable for H_2 generation (0 V vs NHE). In the EC condition, on the other hand, the applied anodic potential (+0.5 V vs Ag/AgCl) makes the H_2 generation unfavored on the cathode as well. On the contrary, a notable H_2 production was observed in the PEC condition where the electrons excited by visible light on the WO_3 film could be effectively transferred to the Pt counter electrode by the potential bias. The presence of dissolved O_2 inhibited the generation of H_2 by scavenging electrons on the cathode (see Figure 8a).[36] However, 4-CP degradation was not retarded at all under an anoxic condition (Ar purging condition), indicating negligible influence of dioxygen on the oxidation reaction. The main oxidants are RCS in this PEC system, and their generation is not hindered by dioxygen because RCS are generated by the direct oxidation of chloride ions with holes. On the other hand, the redox cycle of chloride ions could interfere with the hydrogen evolution. Although the H_2 production rate was slightly dependent on $[Cl^-]$, the average Faradaic efficiency of H_2 evolution was ~100% in the absence of Cl^- and 80% in the presence of Cl^- (based on the measured current, dashed lines in Figure 8b). Anodically generated RCS could be subsequently reduced on the cathode (eqs 15–17), thereby lowering the production efficiency of H_2.

$$HOCl + H^+ + 2e^- \rightarrow Cl^- + H_2O \quad (15)$$

$$Cl\bullet + e^- \rightarrow Cl^- \quad (16)$$

$$Cl_2^{\bullet -} + e^- \rightarrow 2Cl^- \quad (17)$$

Environmental Implications. Water treatment needs energy of which production usually consumes water. Therefore, the development of energy-efficient water treatment technologies helps conserve both water and energy resources. For this purpose, a water treatment process that recovers energy at the same time is an attractive option.[37] A simultaneous production of RCS and H_2 along with the oxidative degradation of organic pollutants (or bacterial inactivation) was demonstrated in this study, employing a WO_3 film photoanode working under visible light. Photon energy drives both the generation of in situ RCS that serves as an oxidant and the production of H_2 as a solar fuel. The present PEC chlorination process has several merits that include no need of catalyst recovery (compared to slurry photocatalysts), an enhanced generation of RCS at relatively low potential bias (+0.7 V vs NHE) compared to the common EC condition (>3.0 V vs NHE),[6,8] and the concurrent production of H_2 for energy recovery. To compare the energy consumption needed to achieve the same level of the target pollutant removal between PEC and EC systems, the degradation of 4-CP was compared between the PEC system (operating at a typical optimized condition of this work: 0.5 V vs Ag/AgCl, 50 mM Cl^-) and a control EC system (employing a BDD electrode biased at 2.0 V vs Ag/AgCl, 50 mM Cl^-). The required energy consumption to achieve 80% removal of 4-CP (50 μM) was estimated to be 49.4 Wh L^{-1} for PEC (WO_3) and 90.2 Wh L^{-1} for EC (BDD) systems, respectively (Figure S10). As long as free sunlight can be employed in the PEC system as a light source, the PEC system consumes much less energy than a typical EC treatment. In addition, it is possible to recover a part of the energy consumed for the chloride activation in the PEC system through the generation of H_2 as a solar fuel. Although the PEC/(visible light) chlorination system was less efficient than the PEC/UV chlorination system, the production of ClO_3^-, a toxic chlorination byproduct, could be inhibited under the visible light irradiation. The presence of Cl^- as a precursor of RCS was essential in the PEC system, and the required concentrations of Cl^- in the 10–50 mM range are ubiquitous in wastewaters. When compared with dark chemical chlorination, the in situ PEC activation of chloride is far more efficient in the mineralization of organic pollutants, which implies that the chlorinated byproducts formation should be reduced as well. However, the efficiency and stability of the present PEC chlorination system employing the WO_3 photoanode are not good enough for practical water treatment applications at the current state and need to be further enhanced with developing more efficient and robust photoanodes and cost-effective reactors.

■ ASSOCIATED CONTENT

Supporting Information

The Supporting Information is available free of charge on the ACS Publications website at DOI: 10.1021/acs.est.9b02401.

Cross-sectional images of WO_3 thin film electrodes, Figure S1; Tauc plot for WO_3 film, Figure S2; cyclic voltammograms of WO_3 thin film electrode, Figure S3; fluorescence emission spectra of HA and FA, Figure S4; current time profiles, Figure S5; time profiles of 4-CP degradation, Figure S6; HPLC analysis of chlorinated intermediates production, Figure S7; time-dependent variation of inactivation of *E. coli* on WO_3 thin film

DOI: 10.1021/acs.est.9b02401
Environ. Sci. Technol. 2019, 53, 9926–9936

electrode, Figure S8; fluorescence emission spectra of 7-HC, Figure S9; time profiles of 4-CP degradation and accompanying current density, Figure S10; and pseudo-first-order rate constant of various pollutants in PEC, PC, and EC conditions, Table S1 (PDF)

AUTHOR INFORMATION

Corresponding Authors

*E-mail: wchoi@postech.edu (W.C.).
*E-mail: antc99@gdut.edu.cn (T.A.).

ORCID

Kangwoo Cho: 0000-0002-1819-7687
Taicheng An: 0000-0001-6918-8070
Wonyong Choi: 0000-0003-1801-9386

Notes

The authors declare no competing financial interest.

ACKNOWLEDGMENTS

This work was supported by the Global Research Laboratory (GRL) Program (NRF-2014K1A1A2041044) and the Framework of International Cooperation program (NRF-2017K2A9A2A11070417), which were funded by the government of Korea (MSIT) through NRF. T.A. acknowledges the financial support from NSFC (41425015 and 41573086) and a part of this work was carried out during W.C.'s visit to Guangdong University of Technology.

REFERENCES

(1) Lin, S. H.; Shyu, C. T.; Sun, M. C. Saline wastewater treatment by electrochemical method. *Water Res.* **1998**, *32* (4), 1059−1066.
(2) Wang, J.; Farrell, J. Electrochemical inactivation of triclosan with boron doped diamond film electrodes. *Environ. Sci. Technol.* **2004**, *38* (19), 5232−5237.
(3) Blatchley, E. R., III; Cheng, M. Reaction mechanism for chlorination of urea. *Environ. Sci. Technol.* **2010**, *44* (22), 8529−8534.
(4) How, Z. T.; Linge, K. L.; Busetti, F.; Joll, C. A. Chlorination of amino acids: reaction pathways and reaction rates. *Environ. Sci. Technol.* **2017**, *51* (9), 4870−4876.
(5) Zanoni, M. V. B.; Sene, J. J.; Selcuk, H.; Anderson, M. A. Photoelectrocatalytic production of active chlorine on nanocrystalline titanium dioxide thin-film electrodes. *Environ. Sci. Technol.* **2004**, *38* (11), 3203−3208.
(6) Park, H.; Vecitis, C. D.; Hoffmann, M. R. Electrochemical water splitting coupled with organic compound oxidation: the role of active chlorine species. *J. Phys. Chem. C* **2009**, *113* (18), 7935−7945.
(7) Weng, S.; Blatchley, E. R., III Ultraviolet-induced effects on chloramine and cyanogen chloride formation from chlorination of amino acids. *Environ. Sci. Technol.* **2013**, *47* (9), 4269−4276.
(8) Cho, K.; Hoffmann, M. R. Urea degradation by electrochemically generated reactive chlorine species: Products and reaction pathways. *Environ. Sci. Technol.* **2014**, *48* (19), 11504−11511.
(9) Sun, P.; Lee, W.-N.; Zhang, R.; Huang, C.-H. Degradation of DEET and caffeine under UV/chlorine and simulated sunlight/chlorine conditions. *Environ. Sci. Technol.* **2016**, *50* (24), 13265−13273.
(10) Minakata, D.; Kamath, D.; Maetzold, S. Mechanistic insight into the reactivity of chlorine-derived radicals in the aqueous-phase UV−chlorine advanced oxidation process: Quantum mechanical calculations. *Environ. Sci. Technol.* **2017**, *51* (12), 6918−6926.
(11) Zhang, H.; Chen, G.; Bahnemann, D. W. Photoelectrocatalytic materials for environmental applications. *J. Mater. Chem.* **2009**, *19* (29), 5089−5121.
(12) Ochiai, T.; Fujishima, A. Photoelectrochemical properties of TiO_2 photocatalyst and its applications for environmental purification. *J. Photochem. Photobiol., C* **2012**, *13* (4), 247−262.
(13) Park, H.; Kim, H.-i.; Moon, G.-h.; Choi, W. Photoinduced charge transfer processes in solar photocatalysis based on modified TiO_2. *Energy Environ. Sci.* **2016**, *9*, 411−433.
(14) Koo, M. S.; Cho, K.; Yoon, J.; Choi, W. Photoelectrochemical degradation of organic compounds coupled with molecular hydrogen generation using electrochromic TiO_2 nanotube arrays. *Environ. Sci. Technol.* **2017**, *51* (11), 6590−6598.
(15) Kim, J.; Lee, C. W.; Choi, W. Platinized WO_3 as an environmental photocatalyst that generates OH radicals under visible light. *Environ. Sci. Technol.* **2010**, *44* (17), 6849−6854.
(16) Kim, H. i.; Kim, H.-n.; Weon, S.; Moon, G.-h.; Kim, J.-H.; Choi, W. Robust co-catalytic performance of nanodiamonds loaded on WO_3 for the decomposition of volatile organic compounds under visible light. *ACS Catal.* **2016**, *6* (12), 8350−8360.
(17) Wang, H.; Lindgren, T.; He, J.; Hagfeldt, A.; Lindquist, S.-E. Photolelectrochemistry of nanostructured WO_3 thin film electrodes for water oxidation: mechanism of electron transport. *J. Phys. Chem. B* **2000**, *104* (24), 5686−5696.
(18) Kim, W.; Tachikawa, T.; Monllor-Satoca, D.; Kim, H.-i.; Majima, T.; Choi, W. Promoting water photooxidation on transparent WO_3 thin films using an alumina overlayer. *Energy Environ. Sci.* **2013**, *6* (12), 3732−3739.
(19) Li, W.; Da, P.; Zhang, Y.; Wang, Y.; Lin, X.; Gong, X.; Zheng, G. WO_3 nanoflakes for enhanced photoelectrochemical conversion. *ACS Nano* **2014**, *8* (11), 11770−11777.
(20) Wang, W.; Wang, X.; Xia, X.-h.; Yao, Z.; Zhong, Y.; Tu, J. Enhanced electrochromic and energy storage performance in mesoporous WO_3 film and its application in bi-functional smart window. *Nanoscale* **2018**, *10*, 8162−8169.
(21) Zheng, H.; Ou, J. Z.; Strano, M. S.; Kaner, R. B.; Mitchell, A.; Kalantar-zadeh, K. Nanostructured tungsten oxide−properties, synthesis, and applications. *Adv. Funct. Mater.* **2011**, *21* (12), 2175−2196.
(22) Gaikwad, N.; Waldner, G.; Brüger, A.; Belaidi, A.; Chaqour, S.; Neumann-Spallart, M. Photoelectrochemical characterization of semitransparent WO_3 films. *J. Electrochem. Soc.* **2005**, *152* (5), G411−G416.
(23) Habazaki, H.; Hayashi, Y.; Konno, H. Characterization of electrodeposited WO_3 films and its application to electrochemical wastewater treatment. *Electrochim. Acta* **2002**, *47* (26), 4181−4188.
(24) Rao, B.; Estrada, N.; McGee, S.; Mangold, J.; Gu, B. H.; Jackson, W. A. Perchlorate production by photodecomposition of aqueous chlorine solutions. *Environ. Sci. Technol.* **2012**, *46* (21), 11635−11643.
(25) Jung, Y. J.; Baek, K. W.; Oh, B. S.; Kang, J.-W. An investigation of the formation of chlorate and perchlorate during electrolysis using Pt/Ti electrodes: The effects of pH and reactive oxygen species and the results of kinetic studies. *Water Res.* **2010**, *44* (18), 5345−5355.
(26) Luo, J.; Hepel, M. Photoelectrochemical degradation of naphthol blue black diazo dye on WO_3 film electrode. *Electrochim. Acta* **2001**, *46* (19), 2913−2922.
(27) Kim, G.; Choi, W. Charge-transfer surface complex of EDTA-TiO_2 and its effect on photocatalysis under visible light. *Appl. Catal., B* **2010**, *100* (1−2), 77−83.
(28) American Public Health Association. *Standard methods for the examination of water and wastewater*, 20th ed.; American Public Health Association: Washington, DC, 1998.
(29) Liu, F.; Chen, X.; Xia, Q.; Tian, L.; Chen, X. Ultrathin tungsten oxide nanowires: oleylamine assisted nonhydrolytic growth, oxygen vacancies and good photocatalytic properties. *RSC Adv.* **2015**, *5*, 77423−77428.
(30) Chakrapani, V.; Thangala, J.; Sunkara, M. K. WO_3 and W_2N nanowire arrays for photoelectrochemical hydrogen production. *Int. J. Hydrogen Energy* **2009**, *34* (22), 9050−9059.
(31) Balitskii, O. A.; Moszyński, D.; Abbas, Z. Aqueous processable WO_{3-x} nanocrystals with solution tunable localized surface plasmon resonance. *RSC Adv.* **2016**, *6* (64), 59050−59054.

DOI: 10.1021/acs.est.9b02401
Environ. Sci. Technol. 2019, 53, 9926−9936

(32) Hill, J. C.; Choi, K.-S. Effect of electrolytes on the selectivity and stability of n-type WO_3 photoelectrodes for use in solar water oxidation. *J. Phys. Chem. C* **2012**, *116* (14), 7612−7620.
(33) Siddiqui, M. S. Chlorine-ozone interactions: formation of chlorate. *Water Res.* **1996**, *30* (9), 2160−2170.
(34) Ishibashi, K.-i.; Fujishima, A.; Watanabe, T.; Hashimoto, K. Detection of active oxidative species in TiO_2 photocatalysis using the fluorescence technique. *Electrochem. Commun.* **2000**, *2* (3), 207−210.
(35) Robert, D. Photosensitization of TiO_2 by M_xO_y and M_xS_y nanoparticles for heterogeneous photocatalysis applications. *Catal. Today* **2007**, *122*, 20−26.
(36) Zhang, B.-T.; Li-Xia, Z.; Jin-Ming, L. Study on superoxide and hydroxyl radicals generated in indirect electrochemical oxidation by chemiluminescence and UV-Visible spectra. *J. Environ. Sci.* **2008**, *20* (8), 1006−1011.
(37) Jeon, T. H.; Koo, M. S.; Kim, H.; Choi, W. Dual functional photocatalytic and photoelectrocatalytic systems for energy and resource-recovering water treatment. *ACS Catal.* **2018**, *8*, 11542−11563.

DOI: 10.1021/acs.est.9b02401
Environ. Sci. Technol. 2019, 53, 9926−9936